A Hierarchical Convolution Neural Network Scheme for Radar Pulse Detection

Van Long Do, Ha Phan Khanh Nguyen, Dat Thanh Ngo and Ha Quy Nguyen
Viettel High Technology Industries Corporation, Hoa Lac High-tech Park, Hanoi, Vietnam

Keywords: Deep Learning, Hierarchical Neural Network, Radar Pulse Detection, Denoising Neural Network.

Abstract: The detection of radar pulses plays a critical role in passive radar systems since it provides inputs for other algorithms to localize and identify emitting targets. In this paper, we propose a hierarchical convolution neural network (CNN) to detect narrowband radar pulses of various waveforms and pulse widths at different noise levels. The scheme, named DeepIQ, takes a fixed-length segment of raw IQ samples as inputs and estimates the time of arrival (TOA) and the time of departure (TOD) of the radar pulse, if any, appearing in the segment. The estimated TOAs and TODs are then combined across segments to form a sequential detection mechanism. The DeepIQ scheme consists of sub-networks performing three different tasks: segment classification, denoising and edge detection. The proposed scheme is a full deep learning-based solution and thus, does not require any noise floor estimation process, as opposed to the commonly used Threshold-based Edge Detection (TED) methods. Simulation results show that the proposed solution significantly outperforms other schemes, especially under severe noise levels.

1 INTRODUCTION

In passive radar systems (Torrieri, 1984; Poisel, 2005), for example, Electronic Intelligence (ELINT) or Early Warning System (EWS), the detection of radar pulses is the process of estimating pairs of the time of arrival (TOA) and the time of departure (TOD) of the pulses from a sequence of received I/Q samples. This task is essential for the location and identification of emitting sources. However, this is not a trivial problem. Nowadays, radar signals are very diversified with various modulation types and pulse widths (Levanon and Mozeson, 2004; Richards, 2014; Pace, 2009). Moreover, in severe conditions with low Signal–to–Noise Ratio (SNR) level, most of radar pulses are buried in noise. Therefore, it is very difficult to detect the presence of true radar pulses in such noisy environments.

In recent years, Deep Learning (LeCun et al., 2015; Goodfellow et al., 2016) has emerged as a powerful tool for many tasks in computer vision and image processing such as image classification (Krizhevsky et al., 2012; Szegedy et al., 2015; He et al., 2016), denoising and image restoration (Zhang et al., 2017; Mao et al., 2016), and object detection (Ren et al., 2017; Redmon et al., 2016; Liu et al., 2016). Inspired by these successes, in this paper, we focus on designing a full deep learning-based scheme, named DeepIQ, for radar pulse detection. In this method, the received radar signal is first divided into overlapping fixed-length segments, each of which is then fed to a hierarchical convolutional neural network to estimate the TOA and/or TOD, if any. By using sufficiently small segments, we can safely assume that each segment contains at most one radar pulse. The TOA and TOD estimates obtained from DeepIQ are tracked and updated, if necessary, after each segment is processed.

The contribution of this paper is as follows:

- We present a novel neural network structure, called Classification Net to determine whether a radar pulse appears in the segment. By using deep-learning based approach, we get rid of noise floor estimation process for setting the detection threshold as in previous works.
- We design a denoising neural network, named Denoising Net to mitigate the noise effect on received radar signal and thus improve significantly the detection accuracy.
- We propose a neural network architecture, named Edge-Detection Net, which contains three different nets (TOA Net, TOD Net and TOA-TOD Net) with the same architecture to estimate the TOA

Do, V., Nguyen, H., Ngo, D. and Nguyen, H.
A Hierarchical Convolution Neural Network Scheme for Radar Pulse Detection.
DOI: 10.5220/0008876500150022
In *Proceedings of the 9th International Conference on Pattern Recognition Applications and Methods (ICPRAM 2020)*, pages 15-22
ISBN: 978-989-758-397-1; ISSN: 2184-4313

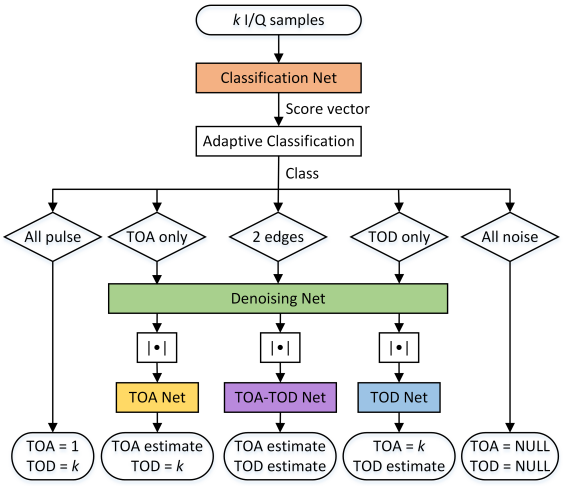

Figure 1: Flowchart of the DeepIQ network.

and/or TOD from the received radar signal depending on the result of the Classification Net.

- We conduct extensive simulations to evaluate the effectiveness of our proposed scheme. The simulation results indicate that DeepIQ improves significantly the radar pulse detection accuracy.

Figure 1 depicts the overview of the DeepIQ scheme. The proposed method receives a segment of k I/Q samples and estimates the TOA and TOD of radar pulses. Our proposed CNN blocks are highlighted in colored. The symbol $|\cdot|$ denotes the modulus operator.

The rest of this paper is organized as follows. We first review the related studies in Section II. In Section III, we describe necessary assumptions and formally define the problem. The detail of our proposed scheme is shown in Section IV. We show simulation results in Section V. Finally, the conclusion is presented in Section VI.

2 RELATED WORK

Since radar pulse detection is an important operation in Electronic Warfare systems such as ELINT or EWS, there are many studies on this problem in recent years. In (Torrieri, 1974; Iglesias et al., 2014), the authors proposed an adaptive thresholding scheme to detect and estimate the TOA and TOD of radar pulses. Albaker *et al.* (Albaker and Rahim, 2011) applied a dual threshold noise gate subsystem to extract the parameters of radar pulses. The authors in (Lakshmi et al., 2013) proposed a model for detection and extraction of pulse parameters in Radar Warning Receivers. In their model, the TOA and TOD are estimated by a predefined hard threshold. In (Lancon et al., 1996), the radar signal is extracted using a correlation method that takes advantage of the periodic characteristic of radar signals. In this method, a detection threshold is selected to determine the correlation peak based on the noise statistic. To the best of our knowledge, all of the aforementioned schemes for radar pulse detection are threshold-based, in which the thresholds are defined through estimating the noise statistics. These methods yield good performances under high or moderate SNR levels but fail under low SNR levels. Moreover, the noise floor estimation–an essence of these algorithms–is itself a non-trivial task, especially in quickly varying environments.

In our previous work (Nguyen et al., 2019), we introduced a deep learning based framework to solve radar pulse detection problem. The method consists of two steps. In the first step, a CNN is trained to determine whether a pulse or part of a pulse appears in a segment of the signal. In the second step, TOA and TOD of radar pulses are estimated by finding the change points in the segment via Pruned Exact Linear Time (PELT) method (Killick et al., 2012). Although this method improved significantly the radar pulse detection performance in comparison with other TED methods, it retains drawbacks. Firstly, since the TOA and TOD parameters are found in the second step by solving an optimization problem using classical find–change–point algorithms, the previously proposed scheme is not a full deep learning approach. Secondly, its performance still is degraded remarkably in noisy conditions with very low SNR level. These shortcomings motivate us to propose a novel scheme that is a full deep learning solution and more resilient to noise. It will be shown that the hierarchical convolution neural network scheme proposed in this paper outperforms previous radar pulse detectors, especially in low SNR conditions.

3 PRELIMINARIES

Considering throughout this paper a narrowband radar signals that are sampled at 78.125 Msps and centered around frequency 0. What we receive is a *complex-valued* (or I/Q) signal that is corrupted by an Additive White Gaussian Noise (AWGN):

$$\hat{x}[n] = x[n] + w[n], \quad n \in \mathbb{Z}, \tag{1}$$

where x is a train of rectangular pulses and w is the AWGN. Assuming Nyquist's sampling, each sample of the discrete-time signal corresponds to a period of 12.8 ns. The pulses are of various waveforms and

pulse widths. This work considers 7 types of modulations commonly used in modern radar systems (Levanon and Mozeson, 2004; Richards, 2014; Pace, 2009): Continuous Waveform (CW), Step Frequency Modulation (SFM), Linear Frequency Modulation (LFM), Non-Linear Frequency Modulation (NLFM), Costas code (COSTAS), Barker code (BARKER), and Frank code (FRANK). Assuming furthermore that all pulses are modulated in the basedband over a bandwidth of 20 MHz. The pulse widths largely vary from 0.1 to 400 μs, which corresponds to a range from 8 to 31250 samples. To reduce the effect of noise, the received signal $\hat{x}$ is lowpass-filtered with filter h of bandwidth 20 MHz that results in:

$$\hat{x}_f = h * \hat{x} = h * x + h * w =: x_f + w_f, \qquad (2)$$

where x_f is a smoothed version of the pulse train and w_f is *colored* Gaussian noise.

The location of each pulse is characterized by the TOA (the middle of the rising edge) and the TOD (the middle of the falling edge). Our goal is to estimate the series of TOAs and TODs by looking at consecutive (overlapping) length–k *segment* of $\hat{x}_f$, one at a time. In practice, the radar pulses in a narrowband are well separated in time and so, we can choose k such that at most one pulse is within a segment. From now on, let us assume that the minimum distance between consecutive pulses is 2000 samples and therefore choose k = 2000. For each segment, if a pulse or a part of it appears, DeepIQ outputs a pair of TOA and TOD in terms of sample indices; otherwise it decides that the whole segment is just noise and set both TOA and TOD to null. Note that if a rising edge is missing, TOA is set to 1; if a falling edge is missing, TOD is set to k. The whole process is achieved by training 5 CNNs separately and attaching them together as shown in Figure 1. A list of detected pulses is kept; when a new pulse is detected, it will be merged to the right previous pulse if the distance between them is negligible.

4 PROPOSED SCHEME

In this section, we describe in detail the architecture of the DeepIQ network which consists of five sub-networks, namely Classification Net, Denoising Net, and three Edge-Detection Nets.

In all of them, we introduce the Dense Squeeze-and-Excitation Block (DSEBlock) that is a combination of a DenseBlock (Huang et al., 2017) with the Squeeze-and-Excitation (SE) mechanism (Hu et al., 2018). The DenseBlock enhances the gradient flow in the network and encourages feature reuse, while

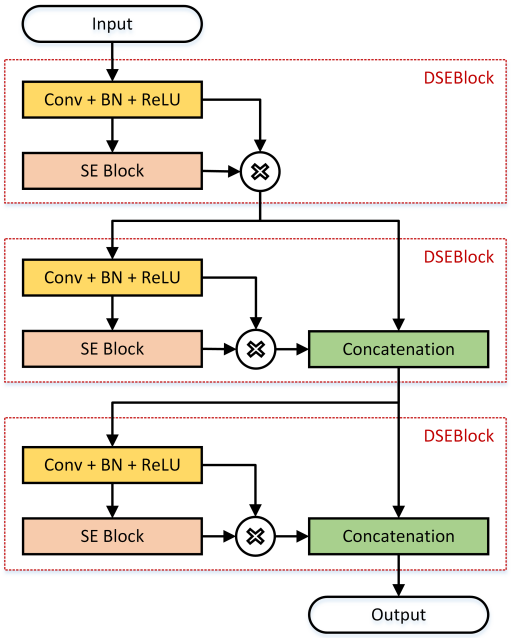

Figure 2: Architecture of DSEBlock-3. DSEBlock-4 and DSEBlock-5 are obtained by repeating the dashed block once or twice more, respectively.

the SE re-weights the feature maps for better feature learning. In a DSEBlock-n, the input is first fed to a composite function consisting of a convolution followed by a Batch Normalization (Ioffe and Szegedy, 2015) and then followed by a Rectified Linear Unit (ReLU). The result is then passed to and also gated by an SE block, whose architecture is described in (Hu et al., 2018). This process is repeated n times with skip connections to form a densely connected network. For example, the architecture of DSEBlock-3 is shown in Figure 2.

4.1 Classification Net

By assuming that each segment of 2,000 I/Q samples can contain at most one pulse, we design the Classification Net to classify a segment into one of the five categories:

- '2 edges': both TOA and TOD of a pulse appear in the segment.
- 'TOA only': a TOA appears in the segment without TOD.
- 'TOD only': a TOD appears in the segment without TOA.
- 'All pulse': the whole segment is a part of a pulse.
- 'All noise': the segment contains only background noise.

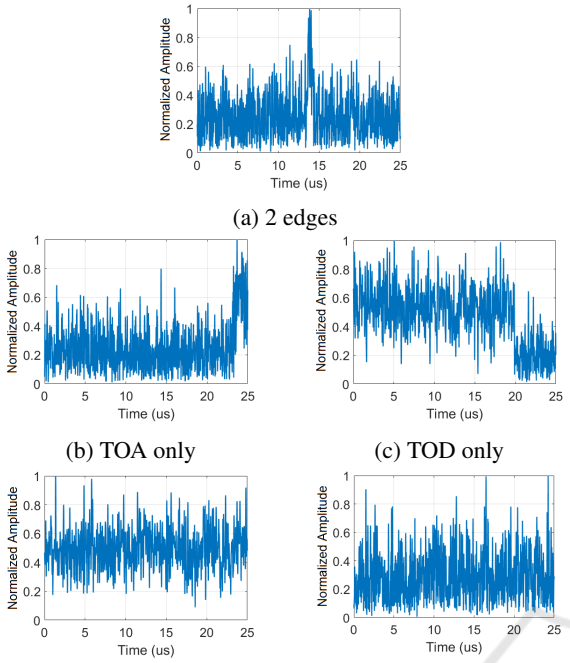

(a) 2 edges

(b) TOA only

(c) TOD only

(d) All pulse

(e) All noise

Figure 3: The 5 classes of segments of the signal envelop for SNR = 6 dB at bandwidth 20 MHz.

Figure 3 depicts these classes under a relatively low–SNR level.

The architecture of the Classification Net is shown in Figure 4. This network consists of a DSEBlock-3 followed by a single filter of size 1×3, a Dropout layer with dropping ratio of 0.5 and 4 fully connected (FC) layers of size 128, 128, 128 and 5, respectively. The first three FC layers use the ReLU activation function, while the last FC layer is attached to a softmax function to output a score vector of length 5. In each convolution layer of the DSEBlock-3, we use 16 filters of size 1×3.

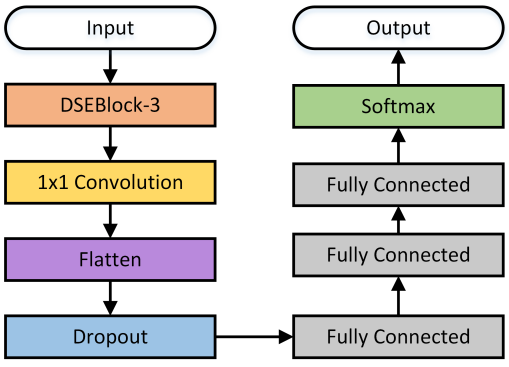

Figure 4: Architecture of the Classification Net.

Each segment s of the signal $\hat{x}_f$ is treated as a 1-D signal with two channels: channel-I (real part) and channel-Q (imaginary part). Before feeding the segment to the Classification Net, we normalize it according to:

$$s_{norm}[n] = \frac{s[n]}{\max_i \max\{|s_I[i]|, |s_Q[i]|\}}, \forall n. \quad (3)$$

The cross-entropy loss function is used to train the network. To decide the label of a segment, we incorporate the score vector output by the Classification Net to an adaptive classification. This procedure takes into account the following observations:(1) '2 edges' cannot be followed by 'All pulse'; (2) 'TOA only' cannot be followed by 'All noise'; (3) 'TOD only' cannot be followed by 'All pulse'; (4) 'All pulse' must be followed by 'TOD only' or 'All pulse' and (5) 'All noise' cannot be followed by 'TOD only' and 'All pulse'. Therefore, the main idea of the adaptive classification is that we exclude impossible labels from the score vector of the current segment based on the label of the previous one, if its confidence was high; then take argument max of the rest as the label and its score as the confidence of the current segment. This is repeated until the end of the signal.

4.2 Denoising Net

We adopt a residual learning strategy (Zhang et al., 2017) for the Denoising Net. The input of the network is a noisy I/Q segment that includes a TOA and/or a TOD and the output is a perturbation of the same size that will be subtracted from the input to compensate for the noise. The network is trained to minimize the mean squared error between the output and the ground-truth noise, which is a segment of w_f given in (2).

The architecture of the Denoising Net is sketched in Figure 5. It incorporates DSEBlocks into an encoder-decoder network with symmetric skip connections (Mao et al., 2016) in the same spirit as (Jégou et al., 2017). Here, we use five DSEBlock-5, each of which is followed by a 1×1 convolution layer to reduce the number of feature maps by a factor of 5. Inside a DSEBlock-5, the number of filters used in the 5 convolution layers are 32, 48, 64, 80 and 96, respectively; all filters are of size 1×7. The Downsampling is simply a 1×2 max pooling. The Upsampling is a 1×7 transposed convolution with stride 2.

4.3 Edge-detection Nets

To locate the edges in a segment, the magnitude of the output of Denoising Net is passed to one of three Edge–Detection Nets: TOA Net, TOD Net and TOA-TOD Net. Which network is used depends on the re-

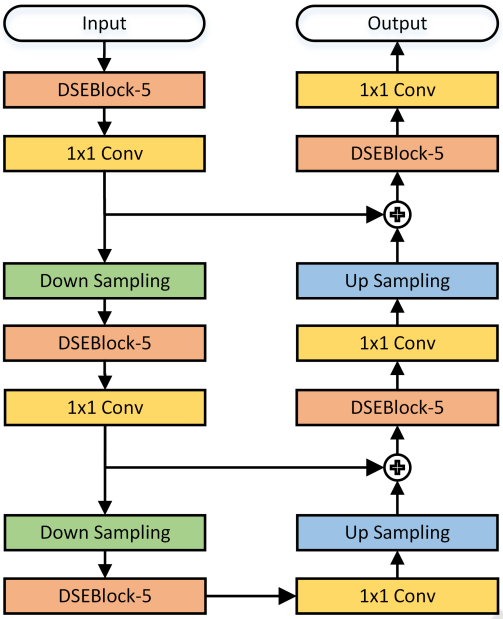

Figure 5: Architectures of the Denoising Net.

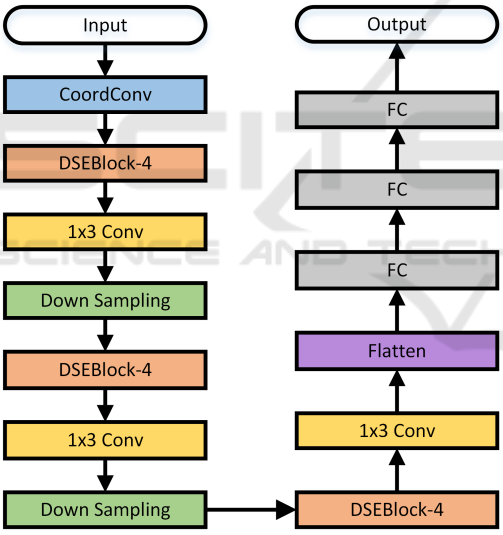

Figure 6: Architecture of the Edge Detection Nets (TOA Net, TOD Net, and TOA-TOD Net). The output of TOA Net or TOD Net is a scalar, whereas the output of TOA-TOD Net is a two-dimension vector.

sult of the segment classification, as shown in Figure 1. These three networks share the same architecture as depicted in Figure 6 but are trained separately on different datasets. The Coordinate-Convolution (CoordConv) layer (Liu et al., 2018) simply maps the coordinates of all samples in the segment to an array in $[-1,1]$ and then appends it to the input as a new channel. This is to incorporate the location information into the learning for better edge detection. The result is then passed to a concatenation of three

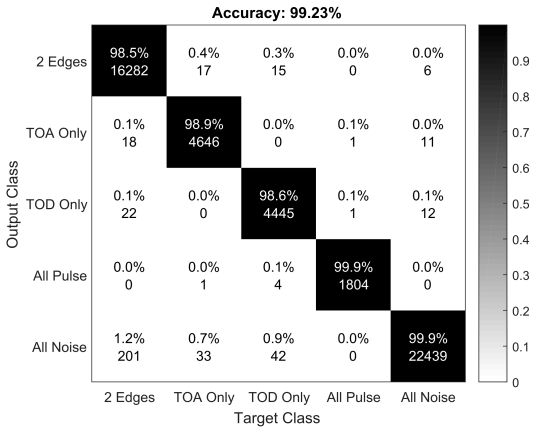

Figure 7: Confusion matrix of Classification Net on the test set.

DSEBlock-4, each of which is followed by a 1×3 convolution layer that reduces the number of feature maps by a factor of 4. The first two of them are further attached to a Downsampling that is a 1×2 max pooling. We use 16, 8 and 4 filters in each convolution layer of the first, second, and third DSEBlock-4, respectively; all filters are of size 1×3.

The tail of the network is a concatenation of 3 FC layers: the first two layers are of size 128 and the last one is of size 1 (for TOA Net and TOD Net) or 2 (for TOA-TOD Net). By using the sigmoid function in the end, the outputs of edge-detection nets are always in $[0,1]$. Each network is trained to minimize the Mean Absolute Error (MAE) between output and ground-truth TOA and/or TOD, which are also normalized to $[0,1]$.

5 PERFORMANCE EVALUATION

In this section, we provide some results for simulated radar pulses. All data were generated by a simulator written in Matlab. The training of proposed sub-networks was implemented in Python with Keras library and TensorFlow backend running on 4 Nvidia Tesla P100 GPUs. The training data for all networks are segments of 2,000 I/Q samples, each of which is randomly truncated from a longer signal that contains a rectangular radar pulse. Each pulse was randomly generated with one of the seven aforementioned modulation types, over a pulse width in $[0.1,400]$ μs and with an SNR (over the 20 MHz bandwidth) in $[0,15]$ dB. All sub-networks were trained for 100 epochs using an Adam optimizer with a learning rate of 10^{-4} and the best models are selected for DeepIQ.

Firstly, the Classification Net was trained on 1,000,000 examples labeled with five categories: '2

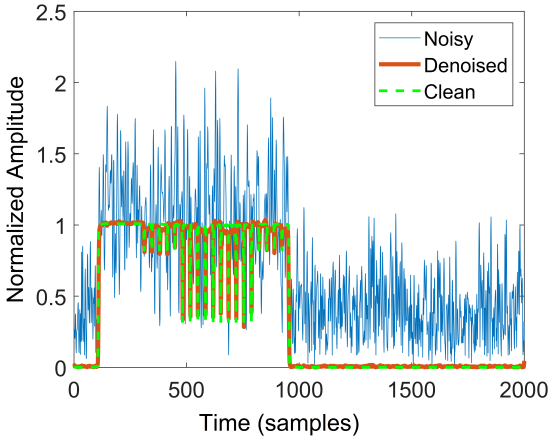

Figure 8: An example of denoising of a modulated radar pulse.

edges', 'TOA only', 'TOD only', 'All pulse' and 'All noise'. The best model was tested on another separated set of 50,000 examples, yielding an overall accuracy of 99.23% with the confusion matrix shown in Figure 7. Secondly, the Denoising Net was trained on 500,000 segments of the first three labels. The resulting model was able to improve the average SNR of 150,000 testing examples by 22.43 dB. Figure 8 visualizes the denoising of an example received noisy radar pulse. Finally, the TOA Net, TOD Net and TOA-TOD Net were trained on three different sets, each of which includes the envelops of 500,000 samples of denoised segments with labels 'TOA only', 'TOD only' and '2 edges', respectively. These networks achieved the MAEs of 26.38 ns, 26.45 ns and 27.67 ns on average, respectively, over separated test sets of 150,000 samples each. To test the whole detection procedure, we run DeepIQ scheme on segments of a long signal containing $N_{true} = 10,000$ pulses equally separated by 6,000 samples under different SNR levels. Two pulses output by DeepIQ are merged into one if the distance between them is less than 25 μs. Then, we evaluate the performance of the proposed DeepIQ network in both detection and estimation metrics.

Let us denote the list of ground-truth TOAs and TODs by $\{(a_i,d_i)\}_{i=1}^{N_{\text{true}}}$ and the list of estimated TOAs and TODs by $\{(\hat{a}_i,\hat{d}_i)\}_{i=1}^{N_{\text{est}}}$. A pulse (a_i,d_i) is called *detected* if there exists $j \in \{1,2,\ldots,N_{\text{est}}\}$ such that:

$$|a_i - \hat{a}_j| < 200\,ns. \tag{4}$$

By renumbering, assuming that the detected pulses $\{(a_i,d_i)\}_{i=1}^{N_{\text{det}}}$ are matched by the subset $\{(\hat{a}_i,\hat{d}_i)\}_{i=1}^{N_{\text{det}}}$ of estimated pulses. The remaining pulses, $\{(\hat{a}_i,\hat{d}_i)\}_{i=N_{\text{det}}+1}^{N_{\text{est}}}$, are considered false alarms. The detection performance is then measured by the following four metrics: the detection rate, the F1 score, the TOA Mean Absolute Error (MAE) and and the TOD MAE, which are computed as:

$$P_d = \frac{N_{\text{det}}}{N_{\text{true}}}, F_1 = \frac{2N_{\text{det}}}{N_{\text{true}} + N_{\text{est}}},$$

$$\Delta_{\text{TOA}} = \frac{1}{N_{\text{det}}} \sum_{i=1}^{N_{\text{det}}} |a_i - \hat{a}_i|,$$

$$\Delta_{\text{TOD}} = \frac{1}{N_{\text{det}}} \sum_{i=1}^{N_{\text{det}}} |d_i - \hat{d}_i|.$$

Note that the detection rate measures the sensitivity of the algorithm while the F1 score balances the true detection rate and the false alarm rate.

To evaluate the performance of our proposed scheme in this paper, we compare the detection accuracy of DeepIQ with that of the Threshold-based Edge Detection (TED) algorithm (Iglesias et al., 2014) and our previous work based on Find–Change–Points algorithms (FCA) (Nguyen et al., 2019). Table 1 reports the detection performances of three methods for various SNR levels from 0 dB to 15 dB. It can be seen that DeepIQ achieves the superior performance compared with TED and FCA in all measures and for all SNR levels. Especially, the performance gaps are strikingly much larger in low-SNR regimes. For example, in the extremely noisy case when SNR = 0 dB, the proposed scheme DeepIQ is able to boost the F1 score from 1.59% of TED and 32.72% of FCA to 55.57%. Furthermore, DeepIQ achieves a reduction of 38 ns and 22 ns in the TOA MAE as compared with TED and FCA. The TOD MAE of DeepIQ is also 27.15 and 6.74 times smaller than that of TED and FCA, respectively.

Our proposed scheme DeepIQ is a better solution to solve the radar pulse detection compared with previous schemes because of the following underlying reasons:

- Firstly, noise floor estimation is a prerequisite in previous TED schemes in order to determine detection threshold. However, in low–SNR levels, accuracy estimation of detection threshold is a very difficult task due to the effect of noise. Improper detection threshold leads to a significant degradation of radar pulse detection, for e.g. high false alarm and missed detection rates. Thanks to the proposed classification neural network with deep-learning approach which reduces the tedious detection threshold setting, DeepIQ reaches a better detection if a radar pulse is present, partially present of absent in the received signal.
- Secondly, previous methods including our previous work apply traditional algorithms such as threshold based algorithm (TED) or find-change-point algorithm (FCA) to estimate the TOA and

Table 1: Performance comparison of schemes with different SNR levels at the bandwidth of 20 MHz.

SNR	Method	Detection Rate	F1 Score	TOA MAE (ns)	TOD MAE (ns)
15 dB	TED	99.72%	**99.84%**	20	29
	FCA	99.24%	99.43%	10	16
	DeepIQ	**99.80%**	**99.84%**	**7**	**15**
12 dB	TED	98.74%	99.20%	22	36
	FCA	97.99%	98.72%	16	19
	DeepIQ	**98.83%**	**99.29%**	**8**	**15**
9 dB	TED	92.48%	94.84%	36	42
	FCA	92.19%	95.14%	28	45
	DeepIQ	**94.58%**	**97.03%**	**12**	**17**
6 dB	TED	56.93%	51.87%	72	2547
	FCA	78.39%	85.03%	44	180
	DeepIQ	**84.98%**	**91.33%**	**19**	**27**
3 dB	TED	12.74%	7.17%	94	12858
	FCA	53.29%	62.66%	59	1331
	DeepIQ	**70.34%**	**81.43%**	**33**	**47**
0 dB	TED	1.78%	1.59%	91	14257
	FCA	24.79%	32.72%	75	3539
	DeepIQ	**42.09%**	**55.57%**	**53**	**525**

TOD positions in the edges of radar pulse. The drawback of these approaches is the edges of radar pulse are deformed critically under the effect of noise in low–SNR levels. Therefore, it is very difficult to estimate correctly in such conditions. By applying the state-of-the art techniques in the proposed Denoising Net and Edge–Detection Nets, DeepIQ can mitigate the effect of noise as well as achieve a significant improvement of detection accuracy in severe conditions.

6 CONCLUSION

In this paper, we have introduced a hierarchical convolution neural network scheme, DeepIQ, for the detection of radar pulses with various waveforms over a wide range of SNR levels. The proposed scheme is obtained by assembling 5 sub-convolution neural network that are in charge of 3 different roles: classification, denoising, and edge detection. These networks are trained on radar I/Q segments of a fixed length. The simulation results show that DeepIQ significantly outperforms the Threshold-based Edge Detection (TED) scheme (Iglesias et al., 2014) and our previous work (Nguyen et al., 2019) especially for low SNR levels. The shortcoming of our method is its computation time, about 0.44 μs/sample on one GPU, which is still far from the real-time target, 12.8 ns/sample. Future work should focus on compressing DeepIQ's sub-networks as suggested in (Han et al., 2016).

REFERENCES

Albaker, B. M. and Rahim, N. A. (2011). Detection and parameters interception of a radar pulse signal based on interrupt driven algorithm. *Int. Conf. on Emerging Research in Computing, Information, Communications and Applications (ERCICA)*, 6:1380–1387.

Goodfellow, I., Bengio, Y., and Courville, A. (2016). *Deep Learning*. MIT Press.

Han, S., Mao, H., and Dally, W. J. (May 02-04, 2016). Deep compression: Compressing deep neural networks with pruning, trained quantization and huffman coding. In *Proc. Int. Conf. Learning Representations (ICLR)*, pages 1–14, Puerto Rico.

He, K., Zhang, X., Ren, S., and Sun, J. (Jun. 27-30, 2016). Deep residual learning for image recognition. In *Proc. Conf. Comput. Vis. Pattern Recogn. (CVPR)*, pages 770–778, Las Vegas, NV, USA.

Hu, J., Shen, L., and Sun, . (June 18-22, 2018). Squeeze-and-Excitation networks. In *Proc. Conf. Comput. Vis. Pattern Recogn. (CVPR)*, pages 7132–7141, Salt Lake City, UT, USA.

Huang, G., Liu, Z., van der Maaten, L., and Weinberger, K. Q. (July 21-26, 2017). Densely connected convolutional networks. In *Proc. Conf. Comput. Vis. Pattern Recogn. (CVPR)*, pages 4700–4708, Honolulu, HI, USA.

Iglesias, V., Grajal, J., Yeste-Ojeda, O., Garrido, M., Sánchez, M. A., and López-Vallejo, M. (May 19-23, 2014). Real-time radar pulse parameter extractor. In *Proc. IEEE Radar Conf.*, pages 1–5.

Ioffe, S. and Szegedy, C. (Jul. 06-11, 2015). Batch normalization: Accelerating deep network training by reducing internal covariate shift. In *Proc. Int. Conf. Machine Learning (ICML)*, pages 1097–1105, Lille, France.

Jégou, S., Drozdzal, M., Vazquez, D., Romero, A., and Bengio, Y. (2017). The one hundred layers tiramisu: Fully convolutional DenseNets for semantic segmentation. arXiv:1611.09326 [cs.CV].

Killick, R., Fearnhead, P., and Eckley, I. A. (2012). Optimal detection of changepoints with linear computational cost. *J. Am. Stat. Assoc.*, 107(500):1590–1598.

Krizhevsky, A., Sutskever, I., and Hinton, G. E. (Dec. 03-08, 2012). Imagenet classification with deep convolutional neural networks. In *Proc. Adv. Neural Inf. Process. Syst. (NIPS)*, pages 1097–1105, Lake Tahoe, NV, USA.

Lakshmi, G., Gopalakrishnan, R., and Kounte, M. R. (2013). Detection and extraction of radio frequency and pulse parameters in radar warning receivers. In *Scientific Research and Essays*, pages 632–638.

Lancon, F., Hillion, A., and Saoudi, S. (1996). Radar signal extraction using correlation. In *European Signal Processing Conf. (EUSIPCO)*, pages 632–638.

LeCun, Y., Bengio, Y., and Hinton, G. (2015). Deep learning. *Nature*, 521:436–444.

Levanon, N. and Mozeson, E. (2004). *Radar Signals*. Wiley-Interscience.

Liu, R., Lehman, J., Molino, P., and Such, F. P. (2018). An intriguing failing of convolutional neural networks and the CoordConv solution. arXiv:1807.03247 [cs.CV].

Liu, W., Anguelov, D., Erhan, D., Szegedy, C., Reed, S., Fu, C.-Y., and Berg, A. C. (Oct. 08-16, 2016). SSD: Single shot multibox detector. In *Proc. Eur. Conf. Comput. Vis. (ECCV)*, pages 21–37, Amsterdam, The Netherlands.

Mao, X.-J., Shen, C., and Yang, Y.-B. (Dec. 05-10, 2016). Image restoration using very deep convolutional encoder-decoder networks with symmetric skip connections. In *Proc. Adv. Neural Inf. Process. Syst. (NIPS)*, pages 1–9, Barcelona, Spain.

Nguyen, H. Q., Ngo, D. T., and Do, V. L. (2019). Deep learning for radar pulse detection. In *Int. Conf. on Pattern Recognition Applications and Methods (ICPRAM)*, pages 32–39.

Pace, P. E. (2009). *Detecting and Classifying Low Probability of Intercept Radar*. Artech House, 2 edition.

Poisel, R. (2005). *EW Target Location Methods*. Artech House.

Redmon, J., Divvala, S., Girshick, R., and Farhadi, A. (Jun. 27-30, 2016). You Only Look Once: Unified, real-time object detection. In *Proc. Conf. Comput. Vis. Pattern Recogn. (CVPR)*, pages 779–788, Las Vegas, NV, USA.

Ren, S., He, K., Girshick, R., and Sun, J. (2017). Faster R-CNN: Towards real-time object detection with region proposal networks. *IEEE Trans. Pattern Anal. Machine Intell.*, 39(6):1137–1149.

Richards, M. A. (2014). *Fundamental of Radar Signal Processing*. McGraw-Hill Education, 2 edition.

Szegedy, C., Liu, W., Jia, Y., Sermanet, P., Reed, S., Anguelov, D., Erhan, D., Vanhoucke, V., and Rabinovich, A. (Jun. 07-12, 2015). Going deeper with convolutions. In *Proc. Conf. Comput. Vis. Pattern Recogn. (CVPR)*, pages 1–9, Boston, MA, USA.

Torrieri, D. J. (1974). Arrival time estimation by adaptive thresholding. *IEEE Trans. Aerospace Electro. Systems*, AES-10(2):178–184.

Torrieri, D. J. (1984). Statistical theory of passive location systems. *IEEE Trans. Aerospace Electro. Systems*, AES-20(2):183–198.

Zhang, K., Zuo, W., Chen, Y., Meng, D., and Zhang, L. (2017). Beyond a Gaussian denoiser: Residual learning of deep CNN for image denoising. *IEEE Trans. Image Process.*, 26(7):3142–3155.